Accepted Manuscript

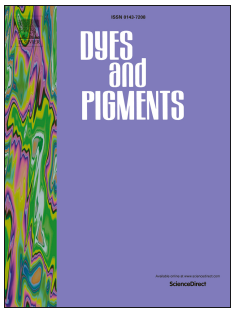

BisBODIPY as PCT-based halogen free photosensitizers for highly efficient excited triplet state and singlet oxygen formation: Tuning the efficiency by different linking positions

Xian-Fu Zhang

PII: S0143-7208(17)31304-9

DOI: 10.1016/j.dyepig.2017.07.051

Reference: DYPI 6140

To appear in: *Dyes and Pigments*

Received Date: 7 June 2017

Revised Date: 11 July 2017

Accepted Date: 21 July 2017

Please cite this article as: Zhang X-F, BisBODIPY as PCT-based halogen free photosensitizers for highly efficient excited triplet state and singlet oxygen formation: Tuning the efficiency by different linking positions, *Dyes and Pigments* (2017), doi: 10.1016/j.dyepig.2017.07.051.

BisBODIPY as PCT-based halogen free photosensitizers for highly efficient excited triplet state and singlet oxygen formation: Tuning the efficiency by different linking positions

Xian-Fu Zhang[a,b,*]

[a] Institute of Applied Photochemistry & Center of Analysis and Measurements, Hebei Normal University of Science and Technology, Qinhuangdao, Hebei Province, China 066004.

[b] MPC Technologies, Hamilton, ON, Canada L8S 3H4.

[*] To whom correspondence should be addressed

E-mail: zhangxianfu@tsinghua.org.cn. Fax: 86 3358387040. Tel: 86 3358387040

Abstract

Four covalent BODIPY hetero-dimers, formed by different linking positions at (2,2'), (2,8'), (3,8') and (8,8') respectively, were designed and synthesized to compare their ability for excited triplet state (T_1) and singlet oxygen generation. In contrast to BODIPY monomers that show negligible photosensitizing ability, the four dimers are very efficient for T_1 and singlet oxygen formation depending on the individual linking style and solvent polarity. Laser flash photolysis, time-resolved/steady state fluorescence, quantum chemical calculation and thermodynamic analysis revealed that the mechanism of triplet state T_1 formation is different from the traditional intersystem crossing mechanism. The T_1 formation is due to charge recombination of the twisted charge separation state (TCSS), while the TCSS is generated by photoinduced intramolecular charge transfer (PCT) from one BODIPY monomer moiety to another within the dimer. The PCT based photosensitizers are also medium polarity sensitive which may be very useful in designing and synthesizing of photosensitizers for photodynamic therapy of tumor, photobiology and organic photochemistry.

Keywords: singlet oxygen; BODIPY dimer; excited triplet state; twisted charge transfer state; laser flash photolysis

1. Introduction

BODIPY (abbreviation for boron-dipyrromethene, the official IUPAC name is 4,4-difluoro-4-bora-3a,4a-diaza-s-indacene) compounds have been advocated as photosensitizers (PSs) in generating excited triplet state and singlet oxygen.[1-3] BODIPYs have high molar absorption coefficients, are environment insensitive, exhibit good resistance to photobleaching, and show higher light–dark toxicity ratios than other PDT agents, these features make them ideal to act as good photosensitizers for PDT.[1-3] Among them, bisBODIPYs (Scheme 1) have been undergoing extensive investigations due to their halogen- and heavy metal-free nature.[4-11] halogen- and heavy metal- contained drugs are not desirable due to the potential harmful side effect. The type of BODIPY dimer PSs is unique because they are able to significantly increase the quantum yields of singlet oxygen formation (Φ_Δ up to 0.90) whereas the corresponding BODIPY monomer compounds show little photosensitizing ability (Φ_Δ<0.10).[5, 9] In addition, the BisBODIPY PSs can be structurally tailored to get high medium polarity selectivity which is a desirable feature for activable PSs in photodynamic therapy of tumors.[7]·[9]

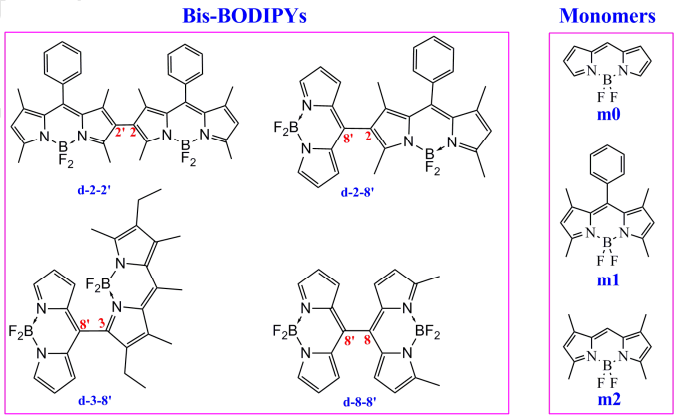

Fig. 1. The chemical structures of BODIPY monomers and dimers in this study.

The bisBODIPY PSs reported are mainly formed by the monomers directly linked at the position (2, 8'), such as d-2-8' shown in Scheme 1. However, a bisBODIPY compound can be synthesized by linking two monomeric BODIPY units at different positions, e.g. 2-2', 2-8', 3-8', and 8-8', as shown in Scheme 1.[12] It is still not clear whether and how the linking position can affect the photosensitizing capability of a bisBODIPY. Although a few types of BODIPY dimers have been examined by us and other authors, each type of them was studied separately from other types and has not been compared under the same condition.[4-11] In this report we compare these different types of BODIPY dimers to understand how their efficiency and mechanism are influenced by the linking positions.

2. Experimental Section

2.1. General

Reagents and solvents for synthesis were used as received from commercial suppliers unless stated otherwise. All reactions were performed in oven-dried or flame-dried glassware unless otherwise stated, and were monitored by TLC using 0.25 mm silica gel plates with UV indicator (60F-254). ^{1}H and ^{13}C NMR are obtained on a 600 MHz Bruker Top Spin NMR spectrometer at room temperature. Chemical shifts (δ) are given in ppm relative to $CDCl_3$ (7.26 ppm for ^{1}H and 77 ppm for ^{13}C) or to internal TMS (0 ppm for ^{1}H). High-resolution mass spectra were obtained on a Thermo Fisher mass spectrometer using APCI-TOF or ESI in positive mode. IR spectra were recorded at room temperature on a Shimadzu FTIR-8900 spectrometer.

UV-visible spectra were recorded on an Agilent 8454 spectrophotometer using 1 cm matched quartz cuvettes. Fluorescence was measured using Edinburgh Instruments FLS920 spectrometer.

All solvents for spectrum, photophysics and DPBF photosensitized oxidation are dried and redistilled according to standard procedures. Details on the measurements for photophysics and singlet oxygen are given in the supporting information.

2.2. Computational simulation

The calculations were carried out using density functional theory (DFT) method as implemented in the Gaussian 09 package. The B3LYP exchange-correlation functional was chosen together with a 6-31G(d) basis set for structural optimization. The solvent effect was modeled using the Polarizable Continuum Model (CPCM) method. In all the cases frequency analysis was made after geometry optimization to ensure the convergence to an energy minimum.

2.3. Synthesis

*2.3.1.**m1** (4,4-difluoro-8-phenyl-1,3,5,7-tetramethyl-4-boron-3a,4a-diaza-s-indacene）*

m1 was prepared according to the general procedure using an aldehyde as a precursor. 50 ml anhydrous dichloromethane (CH_2Cl_2) containing benzaldehyde (2.0 mmol) and 2,4-dimethyl-pyrrole (4.0 mmol) was stirred under argon protection. After 15 min, one drop of trifluoroacetic acid (CF_3COOH) was added, and the solution was

stirred for 12 h at room temperature. Then 2.0 mmol of DDQ (2,3-dichloro-5,6-dicyano-1,4-benzoquinone) was added and the solution was stirred for 30 min. The excess of boron trifluoride diethyl etherate ($BF_3O(Et)_2$, 4 ml) and triethylamine ($N(Et)_3$, 4 ml) was added and stirring was continued for 30 min. The intense fluorescence of reaction mixture was observed on that stage. The formation of intermediates and BODIPY products on every stage was monitored by UV-Vis absorption spectra. After that the reaction mixture was washed with water (100 mL×3), the organic layer was dried over anhydrous $MgSO_4$, filtered and evaporated. The crude product was purified by silica gel chromatography (eluent CH_2Cl_2/hexane=2:1 v/v) to afford pure samples. The product is dark red crystals. Yield: 154 mg, 20 %. mp 127-130 ^oC; IR (KBr)/cm^{-1}: 723, 978, 1072, 1155, 1196, 1471, 1508, 1543 (ν BODIPY ring); 1508, 1543 (ν B-F); 1308, 2854, 2924 (ν CH_3); UV/vis (DCM) λ_{max}/nm: 501; ^1H NMR (600 MHz, Chloroform-d) δ 7.54–7.47 (m, 3H), 7.31–7.28 (m, 2H), 6.00 (s, 2H), 2.58 (s, 6H), 1.39 (s, 6H). HRMS (APCI): m/z calcd for $C_{19}H_{20}BF_2N_2$ $[M+H]^+$ 325.1682, found 325.1682; HRMS (APCI): m/z calcd for $C_{19}H_{19}BFN_2$ $[M-F]^+$, 305.1625, found 305.1623.

2.3.2. ***m2*** *(4,4-difluoro-1,3,5,7-tetramethyl-4-boron-3a,4a-diaza-s-indacene)*

m2 was synthesized by modifying a literature procedure.[14] 250 mL 1,2-dichloroethane was deaerated by bubbling N_2. 2,4-dimethyl pyrrole (1 mL, 11.37 mmol), triethylorthoformate (0.95 mL, 5.69 mmol) and $POCl_3$ (0.58 mL, 6.25 mmol) were added to the deaerated solvent. Reaction was allowed to stir for 2 hours at room

temperature. Then 11.5 mL NEt_3 and 11.5 mL BF_3-etherate were added. After 1 hour the reaction was washed with water (3×250 mL), the organic layer separated, dried on anhydrous $NaSO_4$ and evaporated in vacuo. Column chromatography with $CHCl_3$ as the eluent yielded the pure product as reddish solid (400 mg, 28 %). ^{1}H NMR (600 MHz, Chloroform-*d*) δ 7.07 (s, 1H), 6.07 (s, 2H), 2.55 (s, 6H), 2.27 (s, 6H). ^{13}C NMR (151 MHz, Chloroform-*d*) δ 156.69, 133.35, 120.06, 118.99, 14.67, 11.29.

The dimer **d2-2'**, **d2-8'**, **d3-8'**, and **d8-8'** were prepared by the paths shown in Scheme 1, and the detailed procedure for each compound is given below.

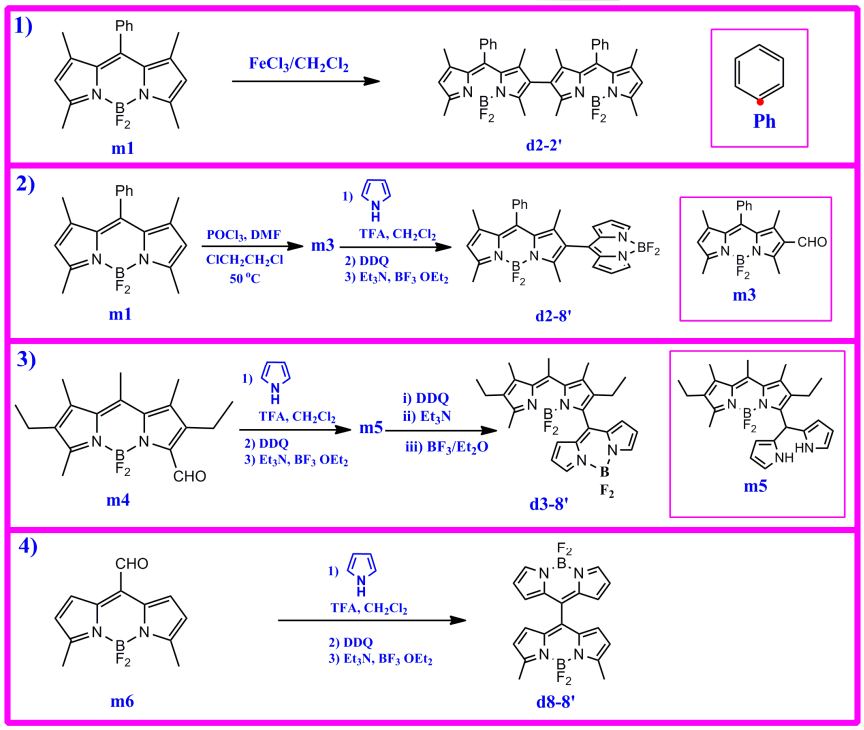

Scheme 1. The synthetic reaction for **d2-2'**, **d2-8'**, **d3-8'**, and **d8-8'**.

*2.3.3. **d2-2'** synthesis*

d2-2' was synthesized by modifying the procedure in reference.[15, 16] $FeCl_3 \cdot 6H_2O$ (245 mg, 0.90 mmol) was refluxed in $SOCl_2$ (2 mL) for 1 h. After $SOCl_2$ was

evaporated under vacuum, dried CH_2Cl_2 (10 mL) containing monomer **1** (130 mg, 0.40 mmol) was added, the resulted solution turned red and then purple immediately from deep green. It was then stirred at 20 ^oC for 30 min, MeOH (10 mL) was added to quench the reaction. The solution was then added to deionized water (100 mL) and stirred for 2 hrs. The organic layer was separated and washed by water three times (3×150 mL), then dried by $MgSO_4$ and filtered. The filtrate was evaporated to give the solid, which was then purified by column chromatography (CH_2Cl_2: petroleum ether = 2: 1). Yield: 7 mg, 6%. IR (KBr)/cm^{-1}: 723, 983, 1084, 1161, 1188, 1357, 1402, 1465, 1514, 1539 (ν BODIPY ring); 1305, 2854, 2924 (ν CH_3); UV/vis (DCM) λ_{max}/nm: 533; HRMS (APCI): m/z calcd for $C_{38}H_{37}B_2F_4N_4$ $[M+H]^+$ 647.3135, found 647.3134; HRMS (APCI): m/z calcd for $C_{38}H_{36}B_2F_3N_4$ $[M-F]^+$ 627.3078, found 627.3078. ^1H NMR (600 MHz, Chloroform-d) δ 7.52 (ddd, 2H, J = 9.3, 4.5, 2.4 Hz), 7.49 – 7.47 (m, 3H), 7.33 (d, 2H, J = 7.5 Hz), 7.27 (dt, 3H, J = 4.3, 2.3 Hz), 6.01 (s, 2H), 2.58 (s, 6H), 2.37 (s, 6H), 1.39 (s, 6H), 1.14 (s, 6H). ^{13}C NMR (151 MHz, Chloroform-d) δ 155.99, 154.68, 143.62, 141.68, 141.22, 135.04, 131.75, 131.24, 129.28, 129.14, 129.02, 127.95, 127.83, 124.73, 121.47, 14.68, 14.44, 13.34, 12.88.

*2.3.4. Synthesis of **d2-8'***

Compound **m3** was synthesized by the procedure in our previous report.[5] Under ice bath, DMF (7.5 mL) in 100 mL three-necked round bottom flask was saturated by N_2 with bubbling the gas for 20 min, $POCl_3$ (7.5 mL) was added drop wise with stirring in 5 min. Ice bath was then removed, and the resulted solution was stirred at room temperature for 20 min. which resulted in a white sticky mixture. Monomer **m1** (194 mg, 0.6 mmol) in 1,2-$ClCH_2CH_2Cl$ (70 mL) was added drop wise into the white mixture, it was then stirred for 6 hrs. at 50 ^oC. After cooling down, the solution was

added drop wise into saturated $NaHCO_3$ aq. solution (400 mL) with stirring for 30 min. The organic layer was extracted by dichloromethane, washed by water (2×200 mL), dried by $MgSO_4$ and filtered. Red solid was obtained after evaporating the filtrate under vacum. The crude compound **m3** was purified by column chromatography (eluent CH_2Cl_2: n-hexane = 2: 1). Yield, 180 mg, 85%. Then **d2-8'** was prepared. CH_2Cl_2 (10 mL, redistilled and dried) containing compound **m3** (62 mg, 0.18 mmol) was saturated by N_2 with bubbling the gas for 30 min. Pyrrole (2 mL, 2.80 mmol) and trifluoro acetic acid (9 μL, 0.12 mmol) were added, the resulted solution was stirred at room temperature for 4 hrs. NaOH aqueous solution (0.2 M, 30 mL) was added to quench the reaction. The organic layer was extracted by dichloromethane, washed by water (2×200 mL), dried by excessive $MgSO_4$ and filtered. The filtrate was added by p-chloranil (60 mg, 0.24 mmol) and stirred for 1 h at room temperature, then triethyl amine (1 mL, 7.12 mmol) was put in under ice bath. After the disappearance of white smog, BF_3-etherate (1 mL, 7.77 mmol) was added, and the resulted solution was stirred at room temperature for 3hrs. 100 mL water was added, and the organic layer was extracted by dichloromethane, washed by water (2×200 mL), dried by $MgSO_4$, filtered, and evaporated by rotavapor. The crude compound was purified by column chromatography (eluent CH_2Cl_2: n-hexane = 1: 1). Dark red solid, yield: 10 mg, 11%. mp 220-223□; IR (KBr)/cm^{-1}: 721, 976, 1074, 1114, 1191, 1263, 1409, 1473, 1508, 1541 (ν BODIPY ring); 1309, 2852, 2924 (ν CH_3); UV/vis (DCM) λ_{max}/nm: 506; HRMS (ESI): m/z calcd for $C_{28}H_{24}B_2F_4N_4Na$ $[M+Na]^+$ 537.2015, found 537.2011; HRMS (ESI): m/z calcd for $C_{28}H_{24}B_2F_3N_4$ $[M-F]^+$ 495.2134, found 495.2131. ^1H NMR (600 MHz, Chloroform-d) δ 8.10 (d, 1H, J = 8.4 Hz), 7.81 (s, 1H), 7.63 – 7.47 (m, 3H), 7.28 (s, 3H), 7.10 (d, 1H, J = 4.4 Hz), 6.87 (d, 1H, J = 8.4 Hz), 6.68 (d, 1H, J = 4.5 Hz), 6.02 (d, 1H, J = 8.7 Hz), 1.60 (s,

6H), 1.28 (s, 6H); ^{13}C NMR (151 MHz, Chloroform-d) δ 155.87, 146.84, 142.64, 140.96, 140.07, 136.25, 135.70, 134.56, 133.56, 133.44, 133.27, 131.71, 131.37, 130.48, 129.33, 128.76, 121.51, 120.04, 15.29, 14.66.

*2.3.5. Synthesis of **d3-8'***

The first step is the synthesis of **m4**. 1,3,5,7,8-tetramethyl-2,6-diethyl BODIPY (64 mg, 0.2 mmol) in THF/H_2O (8/0.08 mL) was titrated drop wisely by THF (2 mL) containing DDQ (180 mg, 0.8 mmol) under ice bath and stirring. The mixture was then stirred for 12 hrs at room temperature. Water (20 mL) was added to quench the reaction. The organic phase was extracted by dichloromethane (3×50 mL), dried (anhydrous Na_2SO_4), and rotavapored. The crude product was purified by column chromatography (300-400 mesh silica, PE/EA = 6:1 v/v) afforded red solid **m4**. Yield 30 mg, 45%. ^{1}H NMR (300 MHz, $CDCl_3$) δ10.29 (s,1H), 2.76 (q, 2H, J=7.0 Hz), 2.72(s, 3H), 2.64 (s, 3H), 2.38 (q, 2H, J=7.5 Hz), 2.34 (s, 3H), 2. 27 (s, 3H), 1.19 (s, 3 H), 1.03 (s, 3H).

The 2nd step is the synthesis of **m5**. m4 (0.5 mmol) was dissolved in pyrrole (5 mL) under argon protection, one drop of trifluoroacetic acid was added, the resulted solution was stirred at r. t. for 0.5 h, then water (20 mL) was added to it. Organic phase was extracted by dichloromethane (3×50 mL), washed by water (3×50 mL), dried by anhydrous Na_2SO_4 and rotavapored. The crude product was purified by column chromatography (300-400 mesh silica, PE/EA = 5:1 v/v) afforded orange solid m5. Yield 67 mg, 30%. ^{1}H NMR (300 MHz, CDCl3) δ 8.51 (s, 2H), 6.68 (s, 2H), 6.27 (s, 3H), 6.16 (s, 2H), 2.62 (s, 3H), 2.52 (s, 3H), 2.44-2.39 (m, 2H), 2.36 (s, 3H),

2.32 (d, 2H, J=7.5 Hz), 2. 27 (s, 3H),1.06 (t, 3H, J=7.4 Hz), 0.50 (t, 3H, J=7.2 Hz). ^{13}C NMR (75 MHz, CDCl3) δ153.4, 151.6, 140.8, 138.3, 137.7, 133.3, 132.5, 132.1, 131.1, 129.0, 116.9, 108.2, 106.6, 36.7, 30.3, 17.4, 17.1, 14. 8, 14.5, 14.3, 13.5, 12.5. HRMS (APCI) calcd. for $C_{26}H_{32}BF_2N_4$ $[M+H]^+$: 449. 2683, found 449.2674.

The 3rd step is **d3-8'** Synthesis. **m5** (0.1 mmol) was dissolved in DCM (10 mL), then DDQ (45 mg, 0.2 mmol) was added under ice bath. 10 min later, triethyl amine (0.8 mL) was added and reacted for 30 min. BF_3-etherate (1 mL) was injected and stirred at r.t. for 4 h. Water (20 mL) was added to quench the reaction. Organic phase was extracted by dichloromethane (3×50 mL), washed by water (3×50 mL), dried by anhydrous Na_2SO_4 and rotavapored. The crude product was purified by column chromatography (300-400 mesh silica, n-hexane/EE = 6:1 v/v) afforded orange solid **d3-8'**. Yield 10 mg, 20%. ^{1}H NMR (600 MHz, Chloroform-*d*) δ 7.92 (s, 2H), 6.89 (d, 2H, *J* = 4.1 Hz), 6.49 (dd, 2H, *J* = 4.2, 1.7 Hz), 2.46 (s, 3H), 2.42 (s, 3H), 2.40 (s, 3H), 2.32 (q, 2H, *J* = 7.5 Hz), 1.27 (s, 3H), 1.03 (t, 3H, *J* = 7.6 Hz), 0.93 (t, 3H, *J* = 7.5 Hz), 0.90 (t, 2H, *J* = 6.9 Hz). ^{13}C NMR (75 MHz, $CDCl_3$) δ 159.6, 144.3, 141.5, 140.2, 138.4, 137.5, 136.3, 135.7, 133.4, 133.1, 131.4, 130.4, 118.2, 17.4, 17.1, 15.5, 14.7, 14.5, 14.2, 13.0. HRMS (APCI) calcd. for $C_{26}H_{28}B_2F_3N_4$ $[M-F]^+$: 475.2452, found 475.2451.

*2.3.6. Synthesis of **d8-8'***

To a mixture of **m6** (40 mg, 0.16 mmol) and pyrrole (2 ml, 28 mmol) in CH_2Cl_2 (10 mL) trifluoroacetic acid (0.021 mL, 0.27 mmol) was added under argon. After the

reaction mixture was stirred at room temperature for 30 min, 0.2 mol/L NaOH (30 mL) aqueous solution was added to quench the reaction. The mixture was extracted with CH_2Cl_2 (3×25mL) and dried (anhydrous Na_2SO_4). Column chromatography (silica, CH_2Cl_2) afforded dipyrromethanes intermediate. A solution of the above dipyrromethane in CH_2Cl_2 (20 ml) was treated with DDQ (125 mg, 0.55 mmol) for 1 hr at room temperature, after the solution was treated with triethylamine (1 ml, 7.2 mmol) for 20 min, boron trifluoride etherate (3 ml, 23.9 mmol) was added and the resulting solution was stirred for 2 hrs at room temperature. The solvent was removed and the reside was column chromatographed (silica, hexane: ethyl acetate = 3:1) to afforded a red solid (13 mg, 20%). ^{1}H NMR (600 MHz, Chloroform-d) δ 7.99 (s, 2H), 7.08 (d, 2H, J = 4.3 Hz), 6.84 (d, 2H, J = 4.3 Hz), 6.55–6.51 (m, 2H), 6.28 (d, 2H, J = 4.2 Hz), 1.29 (s, 6H). ^{13}C NMR (151 MHz, Chloroform-d) δ 159.78, 158.38, 145.74, 134.42, 131.00, 129.73, 123.60, 121.98, 120.17, 118.92, 14.79. HRMS (APCI positive): $C_{20}H_{16}B_2F_3N_4$ $[M-F]^+$ calcd. 391.1513, found 391.1513; $C_{20}H_{17}B_2F_4N_4$ $[M+H]^+$ calcd. 411.1575, found 411.1571.

3. Results and discussion

After the synthesis and purification, the UV-Vis, HRMS, and NMR data were collected, these data are well consistent with the chemical structures of the targeting bis-BODIPYs. To understand the mechanism and the linking position effect on the singlet oxygen formation ability, we carried out a detailed study on their photophysical properties in various solvents.

3.1. UV-Vis absorption spectra

The linking position shows strong influence on the UV-vis absorption spectra (Fig. 2). Compared to the monomer **m1**, all bis-BODIPYs exhibit either red-shifted and broader spectra or a new red-shifted band appeared (**d2-8' and d8-8'**), indicating the J-type electronic coupling between the two components in each BODIPY dimer.

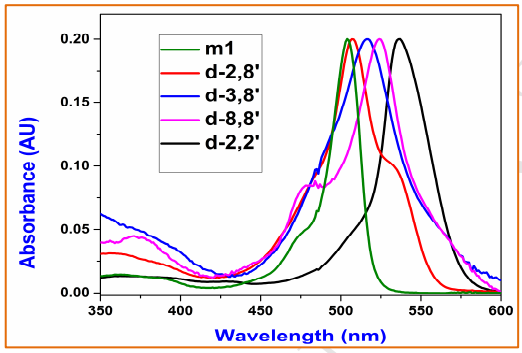

Fig. 2: The normalized UV-vis absorption spectra of BODIPY monomer **m1** and different dimers in air saturated CCl_4 solutions.

The UV-Vis ground state absorption spectra in different solvents for each dimer are shown in Fig. 3. The solvent change (from low to high polarity) showed little effect on the spectra of each bis-BODIPY, so the ground state molecular structures of the bisBODIPYs are little affected by the solvent polarity, i.e. ground state interaction between the monomers in a bisBODIPY is not remarkably changed by the solvent nature.

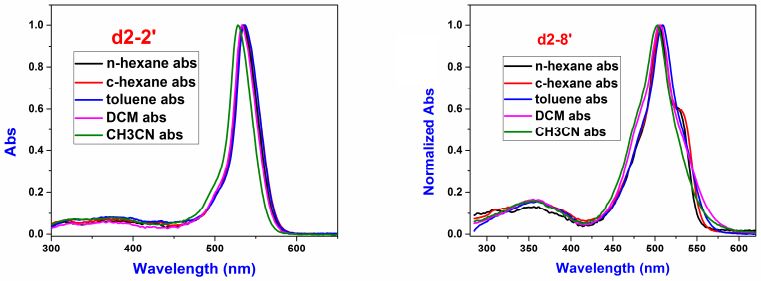

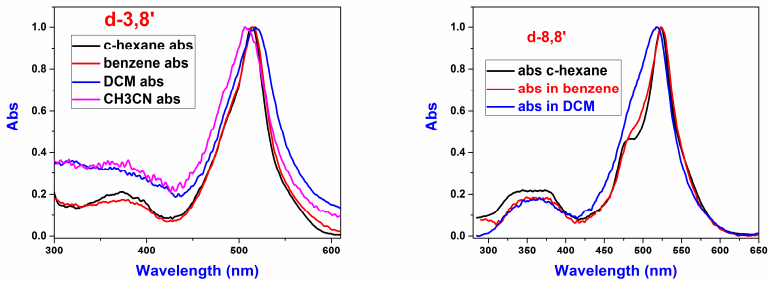

Fig. 3. The UV-Vis absorption spectra of BODIPY dimers in different solvents.

3.2. Fluorescence spectra

The fluorescence spectra of the dimers are displayed in Fig. 4 and compared to that of the monomer **m1**. **m1** shows the typical spectrum of a BODIPY with the band maximum at ca. 510 nm which is only slightly modified by solvent polarity. In the non polar hexane, all compounds show a single fluorescence band. However, a dimer can exhibit dual fluorescence when the polarity of a solvent is sufficiently high (Fig. 4), for example **d-2,8'** and **d-8,8'** exhibit dual emission in DCM, i.e. a new broad and structureless band appears. The short-wavelength band of the dual fluorescence for a dimer M_1-M_2 (M_1 and M_2 are two linked BODIPY monomers) matches the fluorescence from the local excited state of the dimer (LE band, $[M_1\text{-}M_2]^* \rightarrow [M_1\text{-}M_2] + h\nu'$). The second band of the dual emission (which is broad, structureless and largely red-shifted) has the typical feature of ICT (intra-molecular charge transfer) emission, suggesting the occurrence of following process: $M_1^{\bullet\delta+}\text{-}M_2^{\bullet\delta-} \rightarrow M_1\text{-}M_2 + h\nu''$. An ICT state is formed by PCT (photoinduced intramolecular charge transfer) process (ii) after the light absorption process (i):

(i) $M_1\text{-}M_2 + h\nu \rightarrow M_1^*\text{-}M_2$ or $M_1\text{-}M_2^*$, then

(ii) M_1^*-M_2 or M_1-M_2^* $\xrightarrow{PETorPCT}$ $M_1^{\bullet\delta+}$-$M_2^{\bullet\delta-}$ (δ<1 for PCT, δ=1 for PET).

If a whole electron is transferred, then it is a PET (photoinduced electron transfer) process.

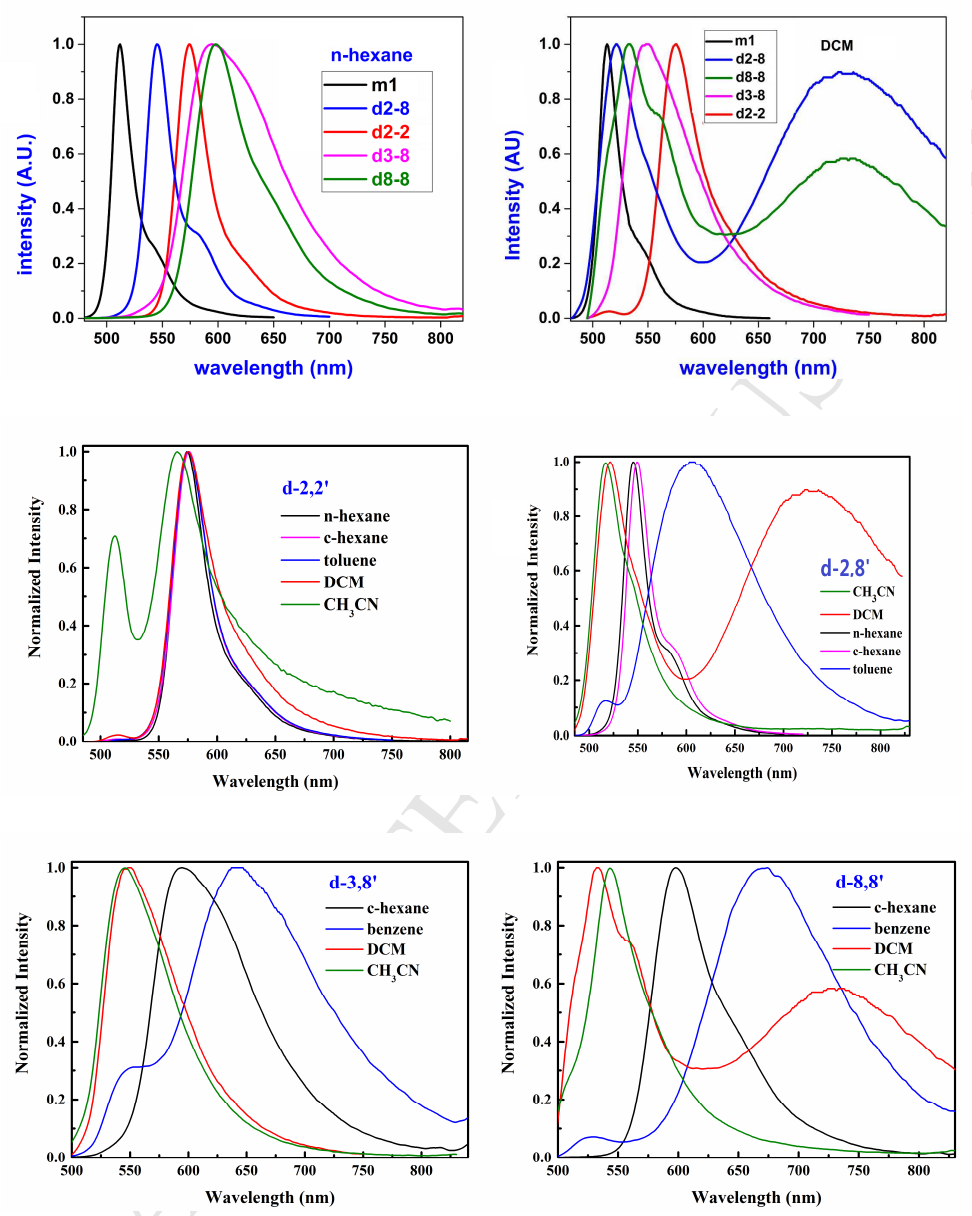

Fig. 4. Top: comparison of fluorescence spectra between monomer **m1** with each dimer. Middle and Bottom: solvent effect on the fluorescence spectra of BODIPY dimers. Ex. Wavelength is 470 nm. The emission is normalized at the emission maximum.

3.3. Fluorescence quantum yield, lifetime and PCT process within a bisBODIPY

Φ_f and τ_f were measured in different solvents (Table 1). The Φ_f value of three dimers (**d-2,8'**, **d-3,8'** and **d-8,8'**) shows the same behavior upon the increase of solvent polarity. Dimer d-2,8', for example, has high Φ_f value in non polar n-hexane (0.81) and c-hexane(0.70), but it decreases sharply in polar solvents, i.e. toluene (0.078), DCM (0.0050), and acetonitrile (0.0033). This strong solvent polarity effect on Φ_f indicates that fast photoinduced charge transfer occurs within a dimer for three dimers (**d-2,8'**, **d-3,8'** and **d-8,8'**): M_1^*-M_2 or M_1-M_2^* $\xrightarrow{PCT}$ $M_1^{\bullet\delta+}$-$M_2^{\bullet\delta-}$, ($0<\delta\leqslant 1$). The dimer **d-2,2'**, on the other hand, shows significant Φ_f decrease only in high polar acetonitrile but not in non or low polar hexane, toluene and DCM.

Table 1. Photophysical data

	Solvent	**λ_{abs} (nm)**	**λ_{em} (nm)**	**Φ_f**	**τ (ns)**	
m1	n-hexane	501	512	0.57	2.76	5.11 (51%)
	c-hexane	503	513	0.48	2.67	5.24 (31%)
	toluene	503	516	0.60	4.04	
	DCM	501	513	0.62	4.28	
	CH_3CN	497	508	0.63	3.97	
m2	c-hexane	508	514	0.96	5.85	
	benzene	510	517	0.90	5.17	
	CH_3CN	501	508	1.00	5.70	
d-2,2'	n-hexane	534	575	0.29	3.79	
	c-hexane	536	576	0.25	3.40	
	toluene	536	519, 575	0.31	3.21	
	DCM	533	516, 575	0.21	3.69	
	CH_3CN	528	512, 566	0.017	0.29	3.71 (12%)
d-2,8'	n-hexane	505	545	0.81	4.31	
	c-hexane	507, 530	549	0.70	4.18	
	toluene	509	517, 610	0.078	1.95	
	DCM	506	526, 740	0.0050	0.53	4.38 (4%)
	CH_3CN	503	517	0.0033	2.13	5.89 (56%)
d-3,8'	c-hexane	515	594	0.34	4.24	
	benzene	516	552, 645	0.045	1.57	4.97 (8%)
	DCM	518	550	0.036	1.88	5.89 (87%)

	CH_3CN	507	546	0.025	1.39	6.29 (90%)
d-8,8'	c-hexane	523	597	0.80	13.5	
	benzene	524	530, 674	0.080	6.07	8.59 (86%)
	DCM	519	534	0.0045	2.36	6.10 (75%)
	CH_3CN	510	543	0.0051	4.27	7.45 (26%)

The fluorescence lifetime (τ_f) of the dimers is also strongly affected by the solvent polarity. The fluorescence decay curves are shown in Fig. 5, from which the fluorescence lifetime values were calculated. **d-2,8'**, **d-3,8'** and **d-8,8'** shows mono exponential decay only in non polar solvent with τ_f value 4.18, 4.24, and 13.5 ns in c-hexane, respectively. With the increase in solvent polarity, the decay becomes biexponential in DCM and MeCN, the smaller one of the two τ_f values is due to the local excited state M_1^*-M_2 or M_1-M_2^*, the larger one is due to the ICT state $M_1^{\bullet\delta+}$-$M_2^{\bullet\delta-}$. Because PCT is enhanced by solvent of higher polarity, τ_f value of the local excited state in polar solvent (τ_f) is significantly smaller than that in non polar solvent (τ_f^0), due to the intramolecular quenching of M_1^* by M_2 or M_2^* by M_1. Therefore the fluorescence decay study supports the conclusion from previous section.

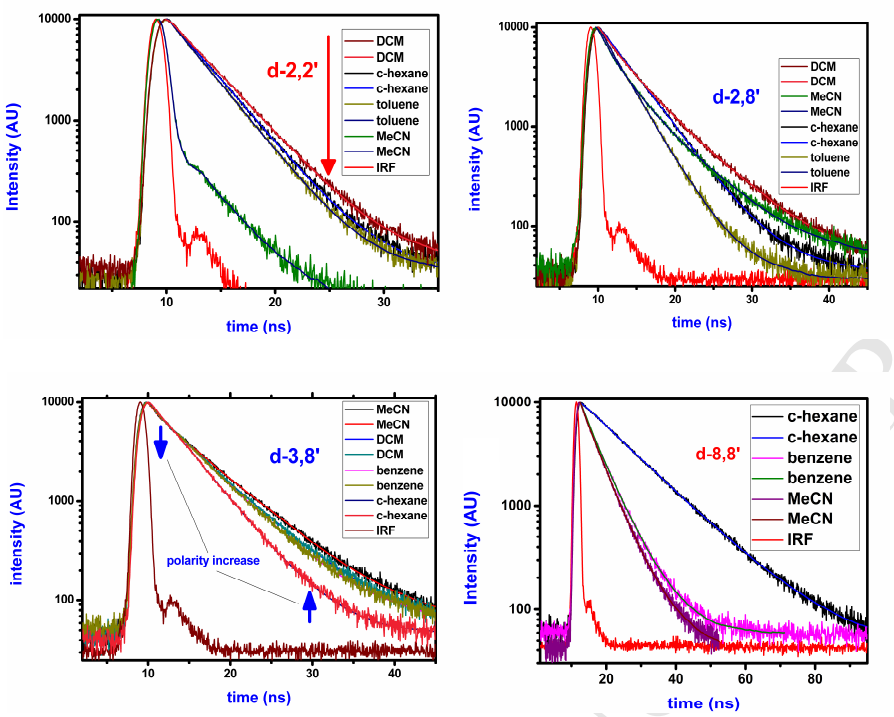

Fig. 5. The fluorescence decay of the dimers in different solvents with excitation at 509 nm (70 ps diode laser), the emission was monitored at fluorescence peak maximum of LE state.

3.4. Geometry of the bisBODIPYs calculated from quantum chemical methods

We calculated their optimal geometry and show them in Fig. 6. Apparently, these covalent dimers are all formed by the head-to-head linking of two planar π-systems, and belong to the J-type dimers according to molecular exciton theory.[17] The dihedral angle θ in the dimer is 67.5° (**d2-2'**), 62.9° (**d2-8'**), 70.0° (**d8-8'**), and 73.2° (**d3-8'**), respectively. The average θ is 68.4 ($\pm$ 5.5) °, indicating these compounds have the similar orientation between the two BODIPY units within a dimer.

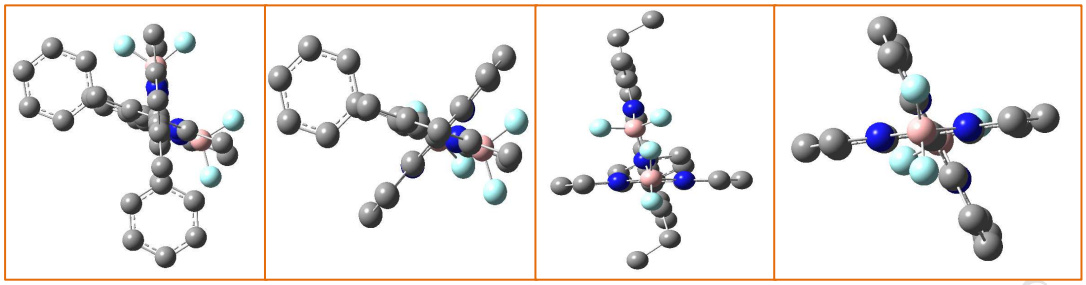

Fig. 6: optimized dimer structures that show the change of the dihedral angle from **d2-2', d2-8', d3-8'** to **d8-8'** (left to right), H atoms are hidden for clear viewing. Structural optimization were carried out by Gaussian 09 on DFT B3LYP/6-31G level with toluene as solvent (cpcm model). The calculated dihedral angle in the dimers: 67.5° (**d2-2'**), 62.9° (**d2-8'**), 73.2° (**d3-8'**), 70.0° (**d8-8'**), respectively. Every BODIPY chromophore in a monomer or dimer is strictly planar.

3.5. PCT based on quantum chemical calculation

For the optimal molecular structure calculated by Gaussian09, the HOMO and LUMO are obtained and shown in Fig. 7. For example, the HOMO of **d-2,8'** is located on the **m1** moiety, while the LUMO is mainly on the **m2** unit, which means that upon deexcitation of S_1 state one electron will be transferred from **m2** unit to **m1** moiety. So are the cases for **d-3,8'** and **d-8,8'**. However, both the HOMO and LUMO of **d-2,2'** are equally distributed on two moieties, indicating that PCT is very difficult to occur, and ICT state is not formed, so that T_1 is very difficult to form. This quantum chemical result is consistent with the previous study.

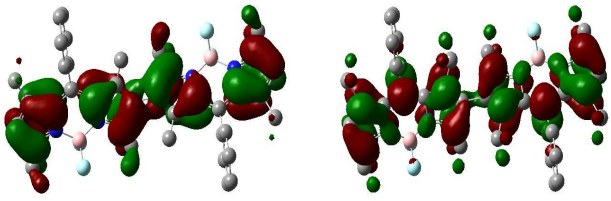

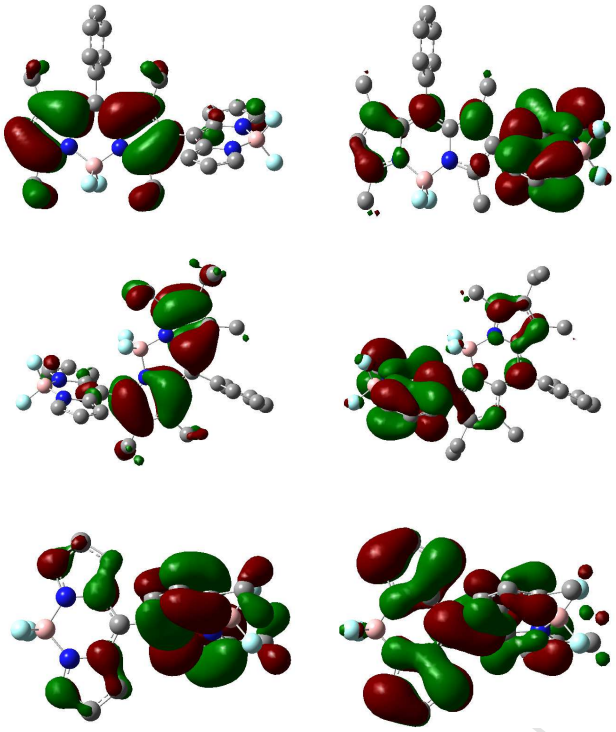

Fig. 7. HOMO, LUMO of **d2-2'**, **d2-8'**. **d3-8'**, and **d8-8'** in acetonitrile from Left to Right , Top to Bottom.

3.6. Identification of singlet oxygen from NIR luminescence

Fig. 8 shows the NIR luminescence spectra with excitation at 505 nm. An emission band at 1270 nm was observed for all the bis-BODIPYs in air saturated solutions, their signal intensity is much higher than that of **m1**. The emission decay at 1270 nm after the excitation pulse was used to obtain the lifetime which has the value 59 ms.[18] The spectral shape and the lifetime value are consistent with that of singlet oxygen ($^1\Delta_g$) reported in literature, this result and the high signal intensity indicate that the four dimers have good ability to produce singlet oxygen. Apparently **d-2,8'** and **d-8,8'** have much higher intensity than **d-3,8'** and **d-2,2'**, suggesting the linking position has a strong effect on the photosensitizing capability of a bisBODIPY. Even the weakest PS **d-2,2'** still shows much stronger signal than the monomer **m1**,

indicate that the covalent dimerization can very significantly increase the photosensitizing capability of BODIPY compounds.

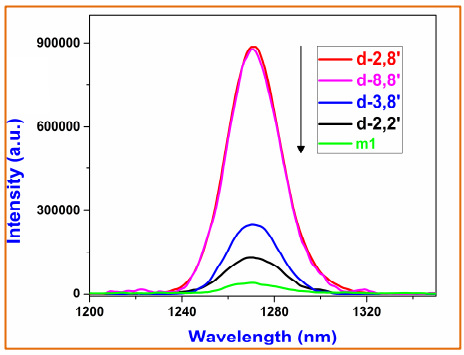

Fig. 8. NIR Luminescence band of singlet oxygen (1270 nm band for $^1\Delta_g$ emission) using different BODIPY monomer **m1** and dimers as photosensitizers in air saturated CCl_4 solutions with excitation at 505 nm (Absorbance is 0.18 at 505 nm).

3.7. Identification of singlet oxygen by DPBF chemical trapping

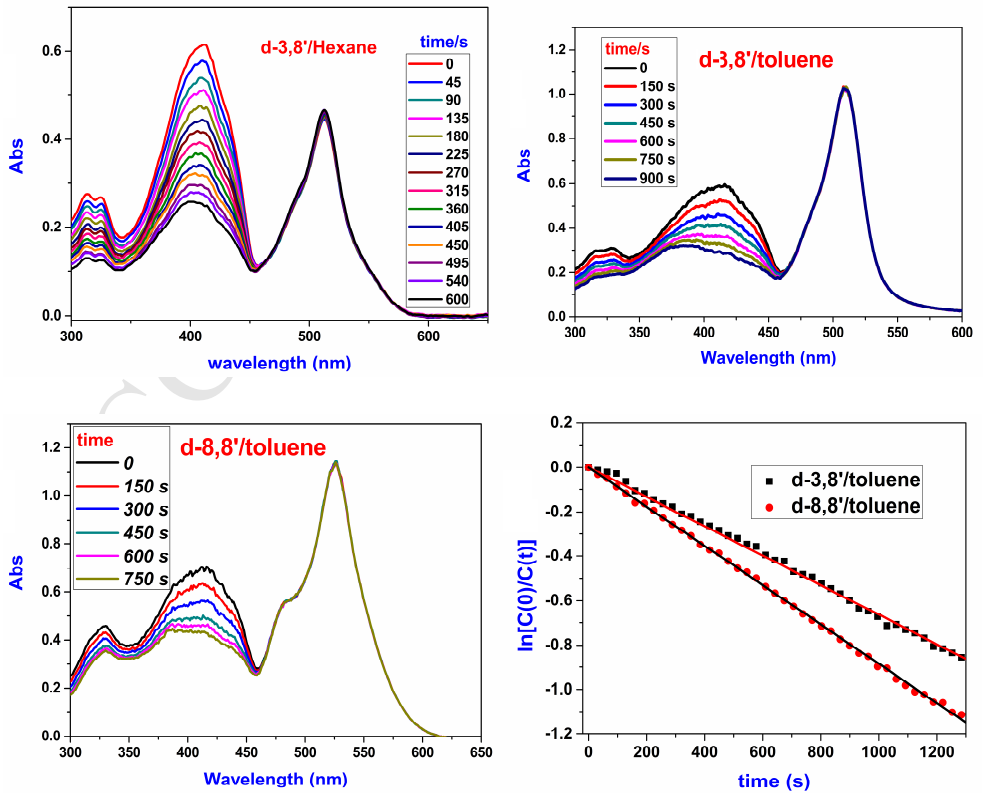

Fig. 9. The change of absorption spectrum upon irradiation time in air saturated solution containing 20 μM DPBF and 5 μM photosensitizer with irradiation at 505 nm. Bottom **Right:** the linear plot of absorbance at 410 nm against irradiation time.

Fig. 9 shows the change of absorption spectra of DPBF (diphenylisobenzofuran) in the presence of BODIPY dimers as photosensitizers in air saturated solutions. The absorption of DPBF decreases quickly with irradiation time, while the absorption peak of the BODIPY photosensitizer showed little change. DPBF is a specific trapper of singlet oxygen, it decomposes upon the reaction with singlet oxygen. The decomposition did not occur in the absence of either a photosensitizer or oxygen, which confirms that BODIPY dimers can really act as photosensitizers.

The formation quantum yield of singlet oxygen (Φ_Δ) was determined for each compound in three solvents and their values are listed in Table 2. In toluene, three dimers with 8'-linkage can generate singlet oxygen in high quantum yield (Φ_Δ is 0.63, 0.81, and 0.87 for **d-3,8'**, **d-2,8'**, and **d-8,8'**), but the Φ_Δ values decreased in solvents with lower polarity, while Φ_Δ of d-2,2' is relatively low in all three solvents. In contrast, the monomers show negligible ability to produce singlet oxygen (Φ_Δ is from 0.023 to 0.083). In most cases, a solvent with higher polarity increases Φ_Δ. Also noticed is that Φ_Δ (d-8,8') > Φ_Δ (d-2,8') > Φ_Δ (d-3,8') > Φ_Δ (d-2,2'), which clearly indicates the linking position effect on Φ_Δ.

Table 2. The formation quantum yield of singlet oxygen

	Toluene	**CCl_4**	**n-Hexane**
d-2,2'	0.053	0.047	0.040
d-2,8'	0.81	0.31	0.19

d-3,8'	0.63	0.076	0.38
d-8,8'	0.87	0.29	0.23
m1	0.065	0.023	0.052
m2	0.083	0.080	0.041

Solvent polarity shows little effect on the absorption spectra of a BisBODIPY (Fig. 3), but has large influence on the formation efficiency of singlet oxygen (Table 2). It can then be concluded that the large solvent effect on $\mathbf{\Phi_\Delta}$ value is due to the excited state interaction between the monomers in a bisBODIPY. The exciton coupling is not the major factor for enhancing the ability in singlet oxygen formation, because **d-2,2'** has the strongest exciton coupling (according to its largest spectral red shift in Fig. 2) but it has the lowest ability to generate singlet oxygen. It is apparent that Φ_f correlates with Φ_Δ, i.e. with the increase in solvent polarity, Φ_f is decreased but Φ_Δ is increased. Since polar solvent enhances PCT, we must conclude that T_1 state is generated from charge separation state: $M_1^{\bullet\delta+}$-$M_2^{\bullet\delta-} \rightarrow M_1(T_1)$-$M_2$ or M_1-$M_2(T_1)$, ($0<\delta\leq1$).

3.8. Triplet excited state generation by the BODIPY dimers

To confirm that $^1O_2$ is truly generated by the photosensitization of the dimers, we identified their excited triplet state (T_1) by laser flash photolysis (LFP). LFP was carried out with excitation at 355 nm (4 ns pulse) in argon and air saturated solutions, respectively. The transient absorption spectra (TAS) are shown in Fig. 10.

BODIPY **m1** and **m2** did not yield well detectable (TAS) within *ns* to *μs* range, i.e. the formation yield of excited triplet state for the BODIPY monomers is too low to be recorded, i.e. ISC (intersystem crossing) from S_1 to T_1 for the monomers are not

efficient. On the other hand, the dimers all show well resolved transient absorption spectra in argon-saturated solution, which are assigned to triplet–triplet (T_1-T_n) absorption as described below.

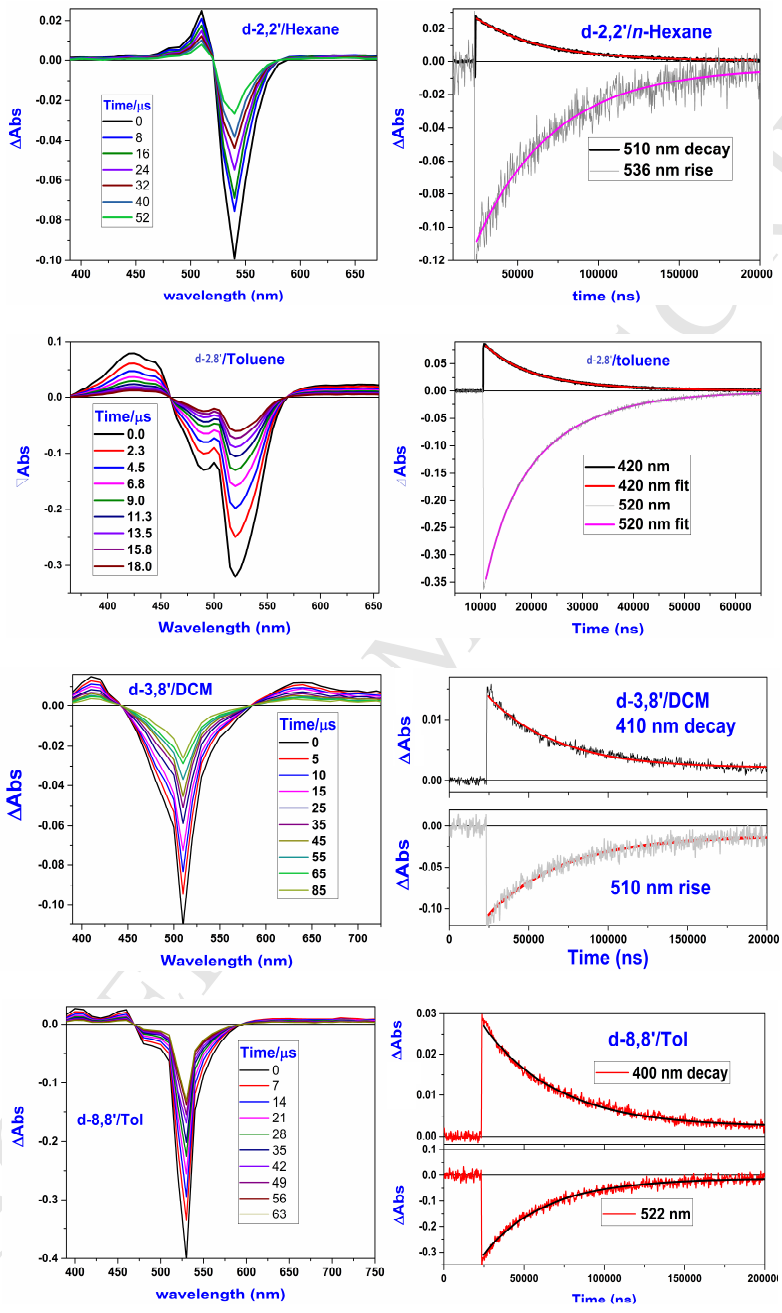

Fig. 10. Transient absorption spectra (**Left**) and the decay of positive transient absorbance (**Right**) in argon purged 20 μM solution, excitation wavelength is 355 nm (4 *ns* Nd:YAG pulsed laser).

All spectra show a positive peak and a negative peak (Fig. 10), and the negative absorption of a dimer matches its ground state absorption. With the decrease in the positive signal (T_1 decay), the negative signal increases (S_0 formation), and the positive bands are separated from the ground state bleaching with well defined isosbestic points. The presence of isosbestic points indicates only two states are involved in the transformation ($T_1 \rightarrow S_0$). These are all the typical spectral behavior of the T_1-T_n absorption. TAS of the bis-BODIPYs differs by their peak position, due to their difference in the absorption of ground state (Fig. 2). The shape and position of the TAS are similar to the T_1-T_n spectra of the BODIPY dyes in previous report.[9] This similarity suggests that the positive signal of is also due to T_1-T_n absorption.

The decay of the positive signal, and the rise of the negative signal, can be well fit by mono exponential function (Fig. 10 right), the rise time and the corresponding decay time are the same, indicating that only one transient species (triplet state T_1) is present in the solutions. The triplet lifetime (τ_T) was computed to be 41 μs for d-2,2', 23 μs for d-2,8', 45 μs for both d-3,8' and d-8,8', which are all long enough for photosensitizing the production of singlet oxygen.

In air saturated solution, the τ_T value is shortened dramatically. For example, τ_T of **d-8,8'** was decreased from 45 to 0.25 μs, τ_T of **d-2,8'** was decreased from 23 to 0.23 μs, but the TAS spectral shape and position were not altered by the presence of oxygen. The rate constant of triplet quenching by oxygen can be then evaluated to be 2.0×10^9 and $2.2\times10^9 M^{-1} s^{-1}$, respectively, which is close to the 1/9 of diffusion rate constant. This effective oxygen quenching also suggests that the positive bands are

indeed due to T_1-T_n absorption. Since TA spectra were not changed by O_2 quenching, the oxygen quenching to T_1 must be a physical process, i.e. $T_1 + O_2 \rightarrow S_0 + {}^1O_2$. In summary, LFP study evidences the T_1 formation for the bis-BODIPYs and the enhancement of T_1 formation by the covalent dimerization.

4. Conclusions

We have synthesized and characterized four BODIPY dimers linked at different positions. We measured the triplet T_1 and singlet oxygen formation properties of the dimers. The tuning of the photosensitizing properties by different linkages are significant, since dimer **d-2,8' and d-8,8'** can generate excited triplet state and singlet oxygen with high quantum yields up to 0.81 and 0.87, respectively, while their corresponding monomer compounds are non photoactive. Based on UV-Vis absorption spectra, we conclude that T_1 formation is from a twisted charge separation state via charge recombination. We show that the photosensitizing efficiency can be tuned not only by the linkage but also by solvent polarity. This photosensitizing mechanism provides a novel strategy for designing efficient and activable photosensitizers which are heavy metal and halogen free and micro-environment sensitive. This type of PCT photosensitizers may find important applications in photodynamic therapy of tumor, photobiology and organic photochemistry.

Acknowledgements

We thank the financial support from Hebei Provincial Hundred Talents Plan (Contract E2013100005), Hebei Provincial Science Foundation (Contract B2014407080) and HBUST (Contract CXTD2012-05).

References

[1] Köksoy B, Kaya EN, Hacıvelioğlu F, Yeşilot S, Durmuş M. Effect of iodine substitution pattern on the singlet oxygen generation and solvent depended keto-enol tautomerization behavior of BODIPY photosensitizers. Dyes and Pigments. 2017;140:384-91.

[2] Mazzone G, Quartarolo AD, Russo N. PDT-correlated photophysical properties of thienopyrrole BODIPY derivatives. Theoretical insights. Dyes and Pigments. 2016;130:9-15.

[3] ünlü H, Okutan E. Preparation of BODIPY- fullerene and monostyryl BODIPY-fullerene dyads as heavy atom free singlet oxygen generators. Dyes and Pigments. 2017;142:340-9.

[4] Cakmak Y, Kolemen S, Duman S, Dede Y, Dolen Y, Kilic B, et al. Designing Excited States: Theory-Guided Access to Efficient Photosensitizers for Photodynamic Action. Angew Chem Int Ed. 2011;50:11937-41.

[5] Pang W, Zhang X-F, Zhou J, Yu C, Hao E, Jiao L. Modulating the singlet oxygen generation property of meso-beta-directly linked BODIPY dimers. Chem Commun. 2012;48(44):5437-9.

[6] Wu W, Cui X, Zhao J. Hetero Bodipy-dimers as heavy atom-free triplet photosensitizers showing a long-lived triplet excited state for triplet-triplet annihilation upconversion. Chem Commun. 2013;49(79):9009-11.

[7] Epelde-Elezcano N, Palao E, Manzano H, Prieto-Castañeda A, Agarrabeitia AR, Tabero A, et al. Rational Design of Advanced Photosensitizers Based on

Orthogonal BODIPY Dimers to Finely Modulate Singlet Oxygen Generation. Chem Euro J. 2017;23(20):4837-48.

[8] Duman S, Cakmak Y, Kolemen S, Akkaya EU, Dede Y. Heavy Atom Free Singlet Oxygen Generation: Doubly Substituted Configurations Dominate S1 States of Bis-BODIPYs. J Org Chem. 2012;77:4516-27.

[9] Zhang X-F, Yang X. Photosensitizer That Selectively Generates Singlet Oxygen in Nonpolar Environments: Photophysical Mechanism and Efficiency for a Covalent BODIPY Dimer. J Phys Chem B. 2013;117:9050-5.

[10] Ventura B, Marconi G, Broring M, Kruger R, Flamigni L. Bis (BF2)-2, 2'-bidipyrrins, a class of BODIPY dyes with new spectroscopic and photophysical properties. New J Chem. 2009;33(2):428-38.

[11] Ozdemir T, Bila JL, Sozmen F, Yildirim LT, Akkaya EU. Orthogonal Bodipy Trimers as Photosensitizers for Photodynamic Action. Org Lett. 2016; 18(19):4821-3.

[12] Momeni MR, Brown A. A Local CC2 and TDA-DFT Double Hybrid Study on BODIPY/aza-BODIPY Dimers as Heavy Atom Free Triplet Photosensitizers for Photodynamic Therapy Applications. J Phys Chem A. 2016;120: 2550-60.

[13] Schmitt A, Hinkeldey B, Wild M, Jung G. Synthesis of the Core Compound of the BODIPY Dye Class: 4,4'-Difluoro-4-bora-(3a,4a)-diaza-s-indacene. J Fluoresc 2009;19:755-8.

[14] Umezawa K, Nakamura Y, Makino H, Citterio D, Suzuki KB. J Am Chem Soc. 2008;130:1550-1.

[15] Nepomnyashchii AB, Bröring M, Ahrens J. Synthesis, photophysical, electrochemical, and electrogenerated chemiluminescence studies. Multiple sequential electron transfers in BODIPY monomers, dimers, trimers, and polymer. J Am Chem Soc. 2011;133:8633-45.

[16] Nepomnyashchii AB, Bröring M, Ahrens J. Chemical and electrochemical dimerization of BODIPY compounds: Electrogenerated chemiluminescent detection of dimer formation. J Am Chem Soc. 2011;133:19498-504.

[17] Kasha M, Rawls H, Ashraf El-Bayoumi M. The exciton model in molecular spectroscopy. Pure App Chem. 1965;11(3-4):371-92.

[18] Grabo WW. Method For Determination Of Singlet Oxygen Quantum Yields For New Fluorene-based Photosensitizers In Aqueous Media For The Advancement Of Photodynamic Therapy. Orlando, Florida: University of Central Florida; 2004.

Supplementary Information

BisBODIPY as PET-based halogen free photosensitizers for highly efficient excited triplet state and singlet oxygen formation: Tuning the efficiency by different linking positions at 2-2', 2-8', 3-8' and 8-8' respectively

Xian-Fu Zhang[a,b,*]

[a] Institute of Applied Photochemistry & Center of Analysis and Measurements, Hebei Normal University of Science and Technology, Qinhuangdao, Hebei Province, China 066004.

[b] MPC Technologies, Hamilton, ON, Canada L8S 3H4.

[*] To whom correspondence should be addressed

E-mail: zhangxianfu@tsinghua.org.cn. Fax: 86 3358387040. Tel: 86 3358387040

Details of Photophysical measurements

The absorption and fluorescence spectra, fluorescence quantum yields and excited singlet-state lifetimes, as well as triplet properties were investigated at room temperature ca 24 ^{o}C. Steady-state fluorescence spectra were acquired on a FLS 920

instrument. All spectra were corrected for the sensitivity of the photo-multiplier tube. The fluorescence quantum yield (Φ_f) was measured by using Eq. (1),[1]

$$\Phi_f = \Phi_f^0 \cdot \frac{F_s}{F_0} \cdot \frac{A_0}{A_s} \frac{n_s^2}{n_0^2}, \qquad \text{Eq. (1)}$$

in which **F** is the integrated fluorescence intensity, **A** is the absorbance at excitation wavelength, n is the refractive index of the solvent used, the subscript 0 stands for a reference compound and s represents samples. Fluorescein was used as the reference (Φ_f^0 = 0.92 in 0.1 M NaOH aq. solution).[2, 3] Excitation wavelengths of 475 nm corresponding to the vibronic band of S_0 to S_1 transitions were employed. The sample and reference solutions were prepared with the same absorbance (A_i) at the excitation wavelength (near 0.09 per cm). All solutions were air saturated for Φ_f measurements.

Fluorescence lifetime of S_1 was measured by time-correlated single photon counting method (Edinburgh FLS920 spectrophotometer) with excitation at 509 nm diode laser (169 ps FWHM) and emission was monitored at emission maximum. Fluorescein was used as the reference (τ_f= 4.16 ns in 0.1 M NaOH aq. solution).[2, 3]

Transient absorption spectra were recorded in degassed solution (prepared by bubbling with Argon for 20 min) with an Edinburgh LP920 laser flash photolysis system. An Nd:YAG laser (Brio, 355 nm and 4 ns FWHM) was used as excitation source. The analyzing light was from a pulsed xenon lamp. The laser and analyzing light beams perpendicularly passed through a quartz cell with an optical path length of 1 cm. The signal was displayed and recorded on a Tektronix TDS 3012B oscilloscope and an R928B detector. The laser energy incident at the sample was attenuated to ca.

10 mJ per pulse. Time profiles at a series of wavelengths from which point by-point spectra were assembled were recorded with the aid of a Pc controlled kinetic absorption spectrometer. Since the observed triplet state lifetimes are dependent on the concentration of a dimer due to the quenching by its ground state, the concentration was adjusted to 20 μM, at which or lower concentration τ_T value is a constant. Under this condition, absorbance at 355 nm A_{355} = 0.25 in a 10 mm cuvettes.

NIR luminescence of singlet oxygen was measured by using InGaAs detector (900-1700 nm) from Edinburgh Instruments with excitation at the absorption maximum (absorbance is 1.0 in 1 cm cuvettes), both excitation and emission are corrected upon the detector response upon light wavelength. Singlet oxygen quantum yield (Φ_Δ) determinations in different solvents were carried out using the chemical trapping method.[4] Typically, a 3 ml portion of the respective PS solutions that contained diphenylisobenzofuran (DPBF) was irradiated at 540 nm in an air saturated solvent. Φ_Δ value was obtained by the relative method using Eq. 2:[4]

$$\Phi_\Delta = \Phi_\Delta^{ref} \frac{k}{k^{ref}} \frac{I_a^{ref}}{I_a}, \qquad \text{Eq. (2)}$$

where Φ_Δ^{ref} is the singlet oxygen quantum yield for the standard (8-methylthio-2,6-diiodoBODIPY, Φ_Δ^{Ref}=0.85, practically independent of the solvent) for excitation at 505 nm),[5] k and k^{ref} are the DPBF photo-bleaching rate constants in the presence of the respective samples and standard, respectively; I_a and I_a^{ref} are the

rates of light absorption at the irradiation wavelength of 540 nm by the samples and standard, respectively. Their ratio can be obtained by Eq. (3).

$$\frac{I_a^{ref}}{I_a} = \frac{1\text{-}10^{-A_{670}^{ref}}}{1\text{-}10^{-A_{670}}}, \qquad \text{Eq. (3)}$$

To avoid chain reactions induced by DPBF in the presence of singlet oxygen, the concentration of DPBF was lowered to ~3×10^{-5} mol dm^{-3}. A solution of sensitizer (absorbance ~0.70 at the irradiation wavelength) that contained DPBF was prepared in the dark and irradiated in the Q-band region. DPBF degradation was monitored by UV-vis absorption spectrum. The error in the determination of Φ_Δ was ~10% (determined from several Φ_Δ values).

References

[1] J. R. Lakowicz, 1 Principles of Fluorescence Spectroscopy, Springer, Singapore, 2006, p. 954.

[2] D. Magde, R. Wong and P. G. Seybold, Photochemistry and Photobiology 2002, 75, 327-334.

[3] X.-F. Zhang, J. Zhang and L. Liu, J. Fluoresc. 2014, 24, 819-826.

[4] F. Wilkinson, W. P. Helman and A. B. Ross, J. Phys. Chem. Ref. Data 1993, 22, 113-262.

[5] N. Epelde-Elezcano, V. Martínez-Martínez, E. Peña-Cabrera, C. F. A. Gómez-Durán, I. L. Arbeloa and S. Lacombe, RSC Adv. 2016, 6, 41991-41998.

Highlights

Four types of bisBODIPYs with different linking positions between monomers were synthesized.

The ability for excited triplet state (T_1) and singlet oxygen generation were compared.

Four dimers are efficient in T_1 and singlet oxygen formation, while their monomers are not.

The linking style and solvent polarity strongly affect the photosensitizing ability of the dimers.

T_1 formation is due to charge recombination of the photoinduced charge transfer state.